

PACS numbers: 42.55.Wd; 42.81.Dp
DOI: 10.1070/QE2015v045n02ABEH015580

Picosecond lasing in ytterbium fibre laser with nonlinear optical loop mirror: experiment and numerical simulation

A.A. Borodkin, D.V. Khudyakov, S.K. Vartapetov

Abstract. **The operation regimes of a pulsed all-normal-dispersion polarisation-maintaining fibre laser with a nonlinear optical loop mirror are studied. The use of polarisation-maintaining fibres ensures polarisation and temperature stability of output radiation. The lasing and instability thresholds of the pulsed laser are determined experimentally. A spectral filter placed in the cavity makes it possible to change the centre wavelength of laser radiation within the range 1.02–1.05 μm with a spectral full width at half maximum of 2 nm. The average output power is 7 mW, which corresponds to a pulse energy of 0.8 nJ. The autocorrelation function width of the output pulse is 50 ps. The minimum pulse duration achieved after compression by an external pair of diffraction gratings is 1.8 ps. The dynamics of the temporal and spectral parameters of laser pulses is studied using mathematical simulation based on numerical solution of the nonlinear Schrödinger equation. The simulation results coincide with experimental data with a high accuracy.**

Keywords: *fibre laser, ultrashort laser pulses, ytterbium, nonlinear optical loop mirror, nonlinear Schrödinger equation.*

1. Introduction

Each year, the field of application of fibre lasers extends and the rate of their commercialisation in many branches of science, engineering and medicine increases. In particular, pulsed fibre lasers are used in fine material processing, engraving and cutting of metals, studying of nonlinear processes, medicine, etc. Undeniable advantages of fibre lasers are their compactness, simple fabrication, high output powers and stable characteristics. One of the promising directions of development of fibre lasers is generation of ultrashort pulses. The normal group velocity dispersion in the case of propagation of a short pulse in a transparent medium leads to temporal and spectral changes of the initial pulse, namely, the pulse broadens in the time domain and a chirp appears in the spectral domain. Most pulsed fibre lasers emit at a wavelength of 1.55 μm, and the problem of pulse dispersion spreading is solved by introduction of fibre segments with anomalous dispersion, which compensate the effect of segments with normal dispersion.

A.A. Borodkin, D.V. Khudyakov, S.K. Vartapetov Physics Instrumentation Center, A.M. Prokhorov General Physics Institute, Russian Academy of Sciences, Troitsk, 142190 Moscow, Russia; e-mail: borodkin_andrey@mail.ru, dimakh65@yahoo.com, svart@pic.troitsk.ru

Received 9 June 2014; revision received 2 September 2014
Kvantovaya Elektronika **45** (2) 98–101 (2015)
Translated by M.N. Basieva

The problem becomes more complicated when the laser wavelength approaches 1 μm. There exist a limited number of methods for obtaining normal dispersion for radiation at this wavelength, namely, the use of microstructured and multimode fibres with anomalous dispersion in the region of 1 μm [1], diffraction gratings in the cavity [2] and chirped fibre Bragg gratings [3]. The use of microstructured fibres is complicated due to considerable problems related to their splicing to a standard fibre. The use of diffraction gratings implies a break in the fibre scheme and optical alignment of a complex compressor scheme. Chirped fibre Bragg gratings are today too expensive and difficult to fabricate. In any of these cases, the fibre laser scheme becomes more complicated, because of which the methods for fabricating pulsed fibre lasers designed only of elements with normal group velocity dispersion are now widely discussed.

Pulsed operation of fibre lasers is obtained using the effect of nonlinear polarisation-ellipse rotation in a single-mode fibre [4, 5], which is characterised both by a variety of pulsed lasing regimes and by instability related to the polarisation state drift due to changes in the external temperature and internal stresses in single-mode fibre. Semiconductor saturable mirrors [6] are difficult to fabricate and are used mainly in linear cavities. The schemes of pulsed lasers with a nonlinear optical loop mirror (NOLM) are designed mainly for non-polarisation-maintaining single-mode passive and erbium active fibres operating at 1.55 μm [7, 8].

An all-fibre 1.03-μm ytterbium pulsed laser based on polarisation-maintaining (PM) fibres with an NOLM is described in [9] (this scheme includes two active elements, one of which is a fibre loop with a gain segment). The presence of a gain element in the loop, on the one hand, allows one to the change the loop radiation parameters in a wide range and thus change the laser operation parameters, but, on the other hand, considerably complicates the laser design.

In this work, we study the operation regimes of a pulsed ytterbium fibre laser with an NOLM without a gain segment in the loop. All elements of the ring fibre laser have normal group velocity dispersion and are polarisation maintaining to achieve polarisation and temperature stability of radiation. The parameters of the fibre mirror as a nonlinear element are varied by changing the fibre length or the ratio of counter-propagating waves in the loop.

2. Scheme of a pulsed laser with a nonlinear optical loop mirror

The scheme of a fibre laser with a nonlinear mirror consisting of elements with normal group velocity dispersion is shown in Fig. 1. The ring laser is made of PM fibres with a core diam-

eter of 6 μm and a cladding diameter of 125 μm. The total ring cavity dispersion is 0.6 ps^2. As an active medium, we used an ytterbium-doped PM fibre with a core diameter of 6 μm and absorption of 250 dB m^{-1} at a wavelength of 975 nm. The active fibre was pumped by a single mode laser diode with a maximum average power of 460 mW at a wavelength of 976 nm. The diode radiation was coupled into the cavity using a PM WDM 980/1030 fibre multiplexor based on a PM fibre. Two output channels (through 20% and 10% couplers) were used to couple out radiation from the cavity and to diagnose the laser radiation, respectively. The linear polarisation in the cavity was oriented along the slow axis of the PM fibre using a fibre isolator–polariser. At the free space part of the laser [segment between collimators (*6*)], the radiation was coupled out into air and coupled into the fibre again with the use of collimators. In the air region, a film spectral filter with a transmission full width at half maximum (FWHM) of 10 nm was placed. Changing the filter inclination angle, it is possible to change the centre wavelength within the range 1.02–1.05 μm. As a mode-locking element, we used an NOLM made of a ring PM fibre segment 13.3 m long. Stable generation of pulses was achieved when using a 90/10 coupler (*3*) in the NOLM loop.

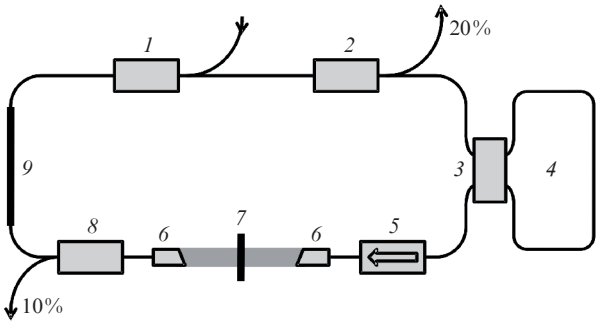

Figure 1. Scheme of the picosecond fibre laser with an NOLM: (*1*) PM WDM 980/1030 multiplexor; (*2*); 20/80 output coupler; (*3*) 10/90 coupler; (*4*) fibre loop 13.3 m long; (*5*) isolator–polariser; (*6*) collimator; (*7*) film spectral filter; (*8*) 10/90 output coupler; (*9*) active fibre.

Since the resonator scheme consisted only of PM fibre elements, pulsed lasing was stable and did not depend on variations in temperature and on bends of optical fibres.

3. Experiment and discussion of results

The upper threshold of stable pulsed operation of the laser was reached at a pump power near 350 mW. After initiation of pulsed lasing, it was possible to decrease the pump diode power to a lower threshold of 200 mW retaining stable pulsed operation. The pulse repetition rate at the chosen cavity length was 8.5 MHz. As the pump power exceeded 350 mW, the laser began to operate in a regime of stochastic pulses.

The average laser output power was 7 mW, which corresponds to a pulse energy of 0.8 nJ. The optical output spectrum in the regime of pulsed operation was measured with a Yokogawa AQ6370C spectrometer with a resolution of 0.5 nm (see Fig. 2). The spectrum of the output pulsed radiation has sharp edges, which indicates that the laser operates in the normal dispersion regime. The centre wavelength and the FWHM of the spectrum were 1048 and 2 nm, respectively. The pulse duration was measured by the method of noncollinear second harmonic generation in a nonlinear crystal, which was used to determine the pulse autocorrelation function (Fig. 3). The FWHM of the autocorrelation function was 50 ps, and the function shape was close to triangular, which testifies that the pulse shape deviated from Gaussian to rectangular.

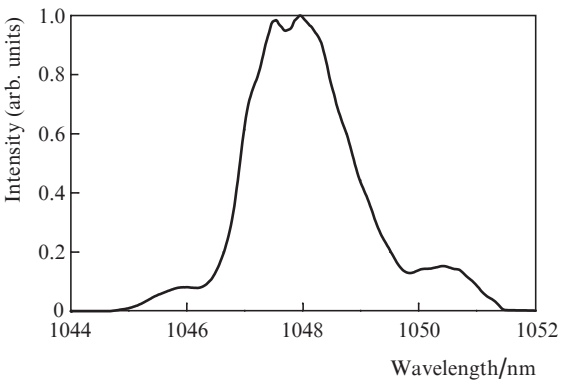

Figure 2. Spectrum of the picosecond fibre laser with an NOLM recorded with a resolution of 0.5 nm.

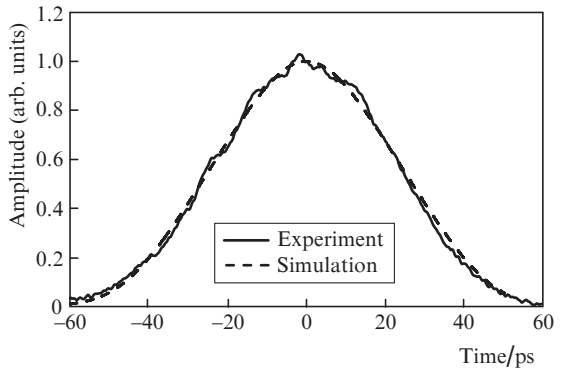

Figure 3. Experimental and calculated autocorrelation functions of uncompressed pulses of the fibre laser with an NOLM.

The output laser pulse was compressed by two diffraction gratings with a line density of 1200 mm^{-1}. The distance between the gratins for optimal compression was 74 cm, which corresponds to an anomalous dispersion of -7.38 ps^2. The compressed pulsed duration was 1.8 ps, which means that the compression coefficient was ~30. The pulses before and after compression are presented for comparison in Figs 3 and 4. The pulse after compression has almost no pedestal, which points to the chirp linearity, as well as to an insignificant contribution of higher dispersion orders and nonlinear self-phase modulation upon pulse propagation through the fibre laser cavity.

The mathematical simulation of the dynamics of temporal and spectral parameters pulses of a fibre laser with an NOLM was performed using the nonlinear Schrödinger equation

$$\frac{\partial A}{\partial z} = \frac{g-\alpha}{2}A - \mathrm{i}\frac{\beta_2}{2}\frac{\partial^2 A}{\partial \tau^2} + \frac{\beta_3}{6}\frac{\partial^3 A}{\partial \tau^3} + \mathrm{i}\gamma |A|^2 A, \qquad (1)$$

where $A(z,\tau)$ is the slowly varying pulse envelope amplitude, which depends on the coordinate z of wave propagation in the

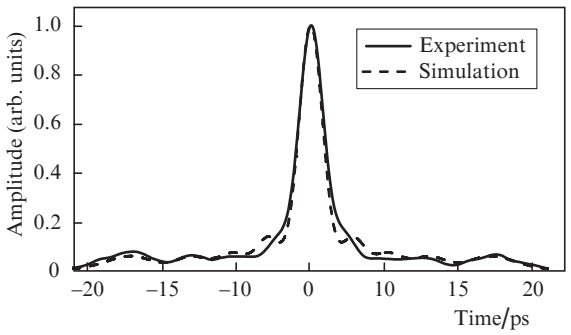

Figure 4. Experimental and calculated autocorrelation functions of compressed pulses.

fibre and on time τ measured in a reference frame moving with the pulse group velocity; g is the gain in the fibre (nonzero only in the active fibre); α corresponds to losses in the fibre; β_2 and β_3 are the group velocity dispersion coefficients of the second and third orders, respectively; and $\gamma = n_2\omega_0/(cA_{\text{eff}})$ is the nonlinear self-phase modulation coefficient (n_2 is the nonlinear refractive index, ω_0 is the central angular frequency, c is the speed of light in vacuum and A_{eff} is the effective beam cross section). The gain saturation effect was not taken into account since the intracavity radiation power was low. The ytterbium gain spectrum was approximated by a Gaussian function with a FWHM of 40 nm and the gain maximum at a wavelength of 1030 nm [10]. The FWHM of the filter transmission spectrum was 10 nm. Deflecting the spectral filter from the normal by a small angle, it was possible to change the centre wavelength from 1.05 to 1.02 μm with a slight decrease in the transmission coefficient in the short-wavelength region. The equation was solved by the standard split-step Fourier method [11].

The calculations were performed for the following fibre parameters: $\beta_2 = 2.5 \times 10^{-26}$ s^2 m^{-1}, $\beta_3 = 2.45 \times 10^{-41}$ s^3 m^{-1}, $\gamma = 4.7 \times 10^{-3}$ W^{-1} m^{-1}. As a fast modulator, we used an NOLM consisting of a coupler with two output channels fused with each other to form a loop (Fig. 5).

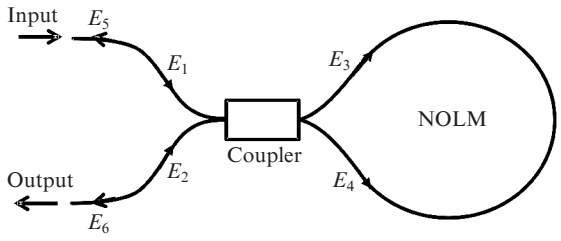

Figure 5. Scheme of a nonlinear loop mirror with the coupler ratio α_0.

The fields characterising an NOLM with a coupler ratio α_0 were found from the expressions [12]

$$E_3 = \alpha_0^{1/2}E_1 + \mathrm{i}(1-\alpha_0)^{1/2}E_2, \tag{2}$$

$$E_4 = \mathrm{i}(1-\alpha_0)^{1/2}E_1 + \alpha_0^{1/2}E_2\,. \tag{3}$$

We calculated the parameters of two counterpropagating waves in the loop (fields E_3 and E_4) and then summed the fields returned to the coupler taking into account formulas (2) and (3). In simulation, we at first intentionally chose a longer pulse than in the experiment with a zero chirp. The calculations were continued until the radiation parameters became unchanged during a number of cavity round-trips. The total normal group velocity dispersion in the fibre cavity was 0.6 ps^2. After several round trips, the combined action of the amplifying medium, self-phase modulation, dispersion, spectral filter and NOLM led to the formation of a stable output pulse (Fig. 6) and a spectrum (Fig. 7) typical for pulsed laser radiation in the case of normal cavity dispersion [13]. The calculated duration of the output chirped pulse was 46 ps (Fig. 6). The pulse autocorrelation function obtained as a result of simulation well agrees with the autocorrelation function measured by the method of noncollinear second harmonic generation (Fig. 3). The pulse shape is close to rectangular, which agrees with the results of other work on pulsed fibre lasers with NOLM [14].

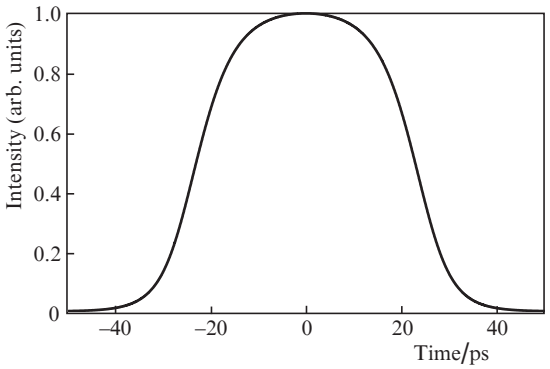

Figure 6. Numerically simulated output pulse of the laser with an NOLM.

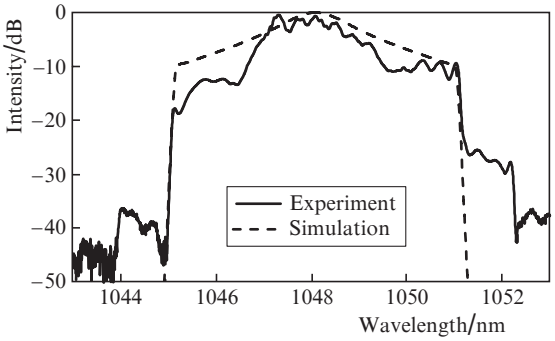

Figure 7. Experimental and calculated spectra of the fibre laser based on an NOLM.

This shape can be easily explained using the dependence of the NOLM loop transmission coefficient on the peak intensity of propagating radiation (Fig. 8) plotted based on the expression [12]

$$K = \frac{|E_6|^2}{|E_1|^2} = 1 - 2\alpha_0(1-\alpha_0)$$

$$\times\left\{1 + \cos\left[(1-2\alpha_0)\,|E_1|^2\,\frac{2\pi n_2 L}{\lambda}\right]\right\}, \tag{4}$$

where K is the loop transmission coefficient, L is the fibre loop length and λ is the radiation wavelength. The peak pulse intensity at the loop input was 0.22 GW cm^{-2} (marked by a dashed line in Fig. 8). The pulse fronts lay in region 1, where the loop worked as a saturable absorber, because of which the fronts became steeper. The pulse top entered region 2, where losses increased with increasing peak intensity, which led to the formation of a flat top of the pulse.

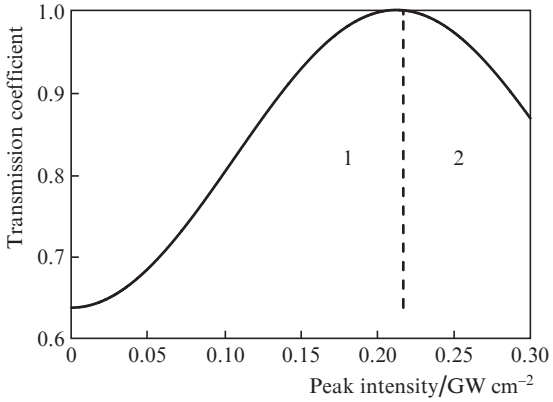

Figure 8. Dependence of the NOLM loop transmission coefficient on the peak intensity of input radiation.

The experimental and calculated spectra of the output pulsed radiation shown in Fig. 7 coincide with each other with a rather high accuracy and have identical FWHMs (2 nm). The minimum pulse duration determined by simulation was 1.5 ps and was achieved at an external anomalous dispersion of -7.3 ps^2, which is rather close to -7.38 ps^2 corresponding to the dispersion of the external compressor in the case of optimal pulse compression. The experimental and calculated autocorrelation functions of the compressed pulse are shown in Fig. 4.

4. Conclusions

A passively mode-locked ytterbium picosecond fibre laser based on a nonlinear optical loop mirror is presented. The cavity scheme is based on fibre with normal group velocity dispersion. The experimental autocorrelation function of the output radiation corresponds to rectangular pulses with a duration of 46 ns. The pulses are linearly chirped and can be compressed by an external compressor to a duration of $\sim$1.8 ps. The pulse repetition rate is 8.5 MHz. The average output power is 7 mW, and the spectral width is 2 nm. The ring cavity is designed using only PM fibres, which ensures a lower sensitivity of the laser to the environmental conditions and a stable polarisation at the exit. Numerical simulation of the pulsed fibre laser shows good coincidence of experimental and theoretical output characteristics.

References

1. Nicholson J.W., Ramachandran S., Ghalmi S. *Opt. Express*, **15**, 6623 (2007).
2. Ilday F.O., Buckley J.R., Lim H., Wise F.W., Clark W.G. *Opt. Lett*., **28**, 1365 (2003).
3. Katz O., Sintov Y. *Opt. Commun*., **281**, 2874 (2008).
4. Kharenko D.S., Podivilov E.V., Apolonski A.A., Babin S.A. *Opt. Lett*., **37**, 4104 (2012).
5. Matsas V.J., Richardson D.J., Newson T.P., Payne D.N. *Opt. Lett*., **18**, 358 (1993).
6. Okhotnikov O., Grudinin A., Pessa M. *New J. Physics*, **6**, 177 (2004).
7. Duling I.N., Chen C.-J., Wai P.K.A., Menyuk C.R. *IEEE J. Quantum Electron*., **30**, 194 (1994).
8. Zhao L.M., Tang D.Y., Cheng T.H., Lu C. *Opt. Commun*., **272**, 431 (2007).
9. Aguergaray C., Broderick G.R., Erkintalo M., Chen S.Y., Kruglov V. *Opt. Express*, **20**, 10545 (2012).
10. Pask H.M., Arman R.J., Hanna D.C., Tropper A.C., Mackechnie C.J., Barber P.R., Dawes J.M. *IEEE J. Sel. Top. Quantum Electron*., **1** (1), 2 (1995).
11. Fisher R.A., Bischel W.K. *Appl. Phys. Lett*., **23**, 661 (1973).
12. Doran N.J., Wood D. *Opt. Lett*., **13**, 56 (1988).
13. Chong A., Renninger W.H., Wise F.W. *Opt. Lett*., **32** (16), 2408 (2007).
14. Ozgoren K., Oktem B., Yilmaz S., Ilday F., Eken K. *Opt. Express*, **19**, 17647 (2011).